

# Computational Quantification of Map Projection Distortion by Fractal Dimension of Coastlines

Franklin Lee

Jericho High School, Jericho, New York, USA

Email: franklin.lee@stonybrook.edu

**How to cite this paper:** Lee, F. (2024)

Computational Quantification of Map Projection Distortion by Fractal Dimension of Coastlines. *Journal of Applied Mathematics and Physics*, 12, 1890-1903.

<https://doi.org/10.4236/jamp.2024.125116>

**Received:** April 23, 2024

**Accepted:** May 27, 2024

**Published:** May 30, 2024

Copyright © 2024 by author(s) and

Scientific Research Publishing Inc.

This work is licensed under the Creative

Commons Attribution International

License (CC BY 4.0).

<http://creativecommons.org/licenses/by/4.0/>



Open Access

## Abstract

Maps, essential tools for portraying the Earth's surface, inherently introduce distortions to geographical features. While various quantification methods exist for assessing these distortions, they often fall short when evaluating actual geographic features. In our study, we took a novel approach by analyzing map projection distortion from a geometric perspective. We computed the fractal dimensions of different stretches of coastline before and after projection using the divide-and-conquer algorithm and image processing. Our findings revealed that map projections, even when preserving basic shapes, inevitably stretch and compress coastlines in diverse directions. This analysis method provides a more realistic and practical way to measure map-induced distortions, with significant implications for cartography, geographic information systems (GIS), and geomorphology. By bridging the gap between theoretical analysis and real-world features, this method greatly enhances accuracy and practicality when evaluating map projections.

## Keywords

Map Projection Distortion, Coastline, Fractal Dimension, Cartography, Geographic Information Systems

## 1. Introduction

Maps, essential tools for portraying the Earth's surface, inherently introduce distortions to geographical features due to how latitude and longitude coordinates map to  $(x, y)$  coordinates on the 2-D plane. Suppose that there exists a perfect 2-D representation of the globe. To test this representation, we draw three line segments on the globe: the equator ( $0^\circ\text{N/S}$ ) from  $0^\circ\text{E/W}$  to  $90^\circ\text{E/W}$ ,

the Prime Meridian from  $0^\circ\text{N/S}$  to  $90^\circ\text{N}$ , and  $90^\circ\text{E}$  from  $0^\circ\text{N/S}$  to  $90^\circ\text{N}$ . These three segments form a triangle where all interior angles are right angles. The sum of the interior angles of all triangles on the 2-D plane that have straight sides is  $180^\circ$ , but the original triangle on the globe, which also has straight sides, has an interior angle sum of  $270^\circ$ , which is a contradiction because our “perfect” 2-D representation of the globe doesn’t preserve angle. We would need to change another property to get three  $90^\circ$  angles at the points where the segments intersect, which would mean that the map projection must change other geometric properties.

Arguably, the most famous attempt to preserve as many geometric properties as possible during projection is the Mercator projection method, which is denoted by  $f(\theta, \phi) = (\theta, \ln(|\sec \phi + \tan \phi|))$ .

This function inputs the longitude  $\theta$  and the latitude  $\phi$  of a point on the globe and outputs  $(x, y)$  coordinates on the Cartesian plane. As  $\phi \rightarrow 90^\circ$ ,  $\tan \theta \rightarrow \infty$  and  $\sec \phi = \frac{1}{\cos \phi} \rightarrow \infty$ , which means that  $\ln(|\sec \phi + \tan \phi|) \rightarrow \infty$  as well, indicating heavy stretching near the poles. Other map projections will have different behavior near the poles. For example, the Lambert Cylindrical Equal-Area projection, which is denoted by  $f(\theta, \phi) = (\theta, \sin \phi)$ , exhibits the opposite effect.

For values  $\phi \approx 90^\circ$ ,  $\sin \phi \approx 1$  using small-angle approximation. As  $\phi \rightarrow 90^\circ$ ,  $\sin \phi$  increases towards 1 very slowly since  $\frac{d}{d\phi} \sin \phi = \cos \phi$ , and when  $\phi \approx 90^\circ$ ,  $\cos \phi \approx 0$ . Since a large change in latitude is required to get a significant change in the  $y$ -coordinate, this map projection shrinks areas near the poles [1].

There are numerous ways to quantify map projection distortion, which are listed in a comprehensive review done by Mulcahy and Clarke. It includes a summary of the most common methods for quantifying map projection distortions, including familiar figures, Tissot’s Indicatrix, and interactive map projections. These methods project different imaginary shapes, such as a human face or an array of circles, spaced at even latitude and longitude intervals [2]. However, these methods do not use geographic data such as coastlines in their analysis. Using fractal dimension to analyze these distortion methods, which analyzes changes in the coastline after projection, would then provide a more practical measurement of projection distortion. The use of fractal dimension calculations on other objects or features before and after projection may also give a more practical assessment of their properties. Fractals have been used in fields like materials science to classify shapes of particles ranging from basalt to concrete to bearing balls. Using image analysis and comparisons between apparent areas and perimeters, a team of researchers led by Seracettin Arasan found that, like coastlines, a particle’s irregularity increases as its fractal dimension increases. This conclusion was supported by the fact that increases in the overall roundness led to decreases in fractal dimension, and increasing angularity of particles led to

increased fractal dimension [3]. To study geology using fractals, independent researcher Qiuming Cheng used a perimeter-area model to study geological data to find differences in the distribution of certain metals such as gold, copper, silver, and arsenic in the Mitchell-Sulphurets district [4].

The fundamental connection between fractals and geometry makes fractal dimension a superior method to measure the properties of geographic features. The first fractals were self-similar figures like the Cantor set and the Koch Snowflake [5] [6]. The fractal dimensions of these figures were defined by how the fractal's size (length, area, volume, etc.) changes with each iteration of a defined process. After these developments, fractal dimensions were generalized beyond basic self-similar shapes. Mathematicians like Benoit Mandelbrot started examining the fractal features of coastlines by walking different pairs of divider gauges, which look like compasses (the mathematical tool), along a stretch of coastline to estimate its length [7]. The estimations are then graphed on log-log axes, on which the base-ten logarithm of the estimation and the base-ten logarithm of the distance between the dividers are correlated. Mandelbrot found that the slope of this log-log graph is  $1 - D$ , where  $D$  is the true fractal dimension of the coastline. Therefore, given a fractal with a dimension in the range  $[1, 2)$  and the distance between the dividers  $L_{\text{gauge}}$ ,  $\log(L_{\text{measured}}) \approx (1 - D)\log(L_{\text{gauge}}) + \lambda$ , where  $\lambda$  is an unknown real number. The value  $\lambda$  cannot be defined precisely because  $\lim_{L_{\text{gauge}} \rightarrow 0} \log(L_{\text{gauge}})$  doesn't have a lower bound, so this method can only extrapolate to reasonable values of  $L_{\text{gauge}}$ , whose bounds depend on the size and complexity of the fractal. The fractal dimension of the coastline could also be estimated by counting the number of boxes that cover a stretch of coastline using different box sizes, and those counts can similarly be used on log-log axes to create a regression line, which Mandelbrot stated as an alternative method, which is easier for computers to handle. The linear relationship is identical to that for the divider method, but  $L_{\text{gauge}}$  is replaced with the grid size. The linear regression model created using this method can also only be extrapolated to reasonable box sizes, as there will be an infinite number of boxes of size 0 covering a stretch of coastline, and there will always be one box covering a stretch of coastline for extremely large box sizes [8]. Mandelbrot further examined the innumerable applications of fractal geometries in nature, delving into the fractal geometries of clouds and mountains [9]. Previous research used these ideas to examine changes in the fractal dimensions of clouds before and after projecting onto a 2-D surface, which means that there should also be a correlation between projections of the globe and the resulting fractal dimensions of specific stretches of coastline [10]. Analyzing distortion using the fractal dimension is more applicable than traditional methods since fractal dimensions can be calculated or used for almost any image including landscapes, a cross-section of the brain obtained from an MRI scan, or a city's expansion patterns [11] [12] [13]. Putting these fundamental methods into practice, a team of researchers led by Akhlaq Husain applied the box-counting method on the coastline of Australia and

found its fractal dimension to be about 1.1430. The paper also stated several practical advantages of using the box-counting method to analyze coastlines, including scalability, flexibility, and general applicability, ranging from coastlines to features of other planets [14].

The existing applications of fractal dimensions in finding differences in shape features could be extended to finding differences in the shapes of continents on various types of map projections. Additionally, with the drastic increase in computational power and the wider availability of accurate and precise datasets like satellite images in the current era, calculating differences in fractal dimension will be quicker, and methods for doing so will constantly improve [15]. The literature above shows that previous researchers on this subject may have forgotten to consider the general applicability of their methods but focused more on the fundamental objectives of their research. It also shows that fractals have an enormous potential for evaluating map projections. Even though previous work has greatly improved the completeness of perceptions about map projections and shapes in general, the connection between these two fields has not been widely researched yet. For instance, when measuring the fractal dimension of coastlines, researchers often do not adequately discuss other factors that may impact their calculations. Map projections are also discussed in a more theoretical sense and may not take landmass features into account. Therefore, the combination of map projections and their analysis methods will not only broaden the applicability of research methods but also facilitate accurate and precise analysis of map projection distortions. Using the advantages of fractal dimensions to analyze map projection distortion can then broaden our view of projection distortion. Not only can this method motivate the development of cartography and other related fields, but it can also supply geographic information systems, sensor technologies, and other regimes with more reliable data.

To specifically analyze the relationship between the fractal dimension of coastlines and map projection distortion, we will use fractal dimension to analyze fixed boxes of size  $512 \times 512$  pixels centered at fixed geographical locations (e.g., the area around Anchorage, Iceland, northern Norway, etc.) before and after projecting to the Mercator projection from the WGS84 equirectangular projection. This is a novel method of analyzing map projection distortion because it isn't purely a technical analysis (e.g. analyses of deformations on Tissot's Indicatrixes) but rather a more qualitative and practical analysis of the distortion in geographical features depicted on a map.

## 2. Materials and Methods

### 2.1. Materials

Below are two Python programs that project the world's coastlines (data from [16]) displayed in the WGS84 coordinate system using different types of projections and process an image at a specified range of x and y coordinates (in a  $512 \times 512$  bounding box) to find its fractal dimension using the box-counting method.

This code below projects OpenStreetMap coastline data into the Mercator, Central Cylindrical, Equal Earth, and Lambert Cylindrical Projections using their respective formulas. We find the minimum and maximum values of the x and y coordinates by plugging in extreme values (90°N or 180°) for latitude and longitude and scaling the map accordingly.

```

from PIL import Image
from math import *

from numpy import arcsin, infity

Image.MAX_IMAGE_PIXELS = 200000000

# Read in "map.png" as a matrix of RGBA values
map = Image.open('Image File Name') # Could be any map
matrix = map.load()
coastline = []
for i in range(20000):
    for j in range(10000):
        if(matrix[i,j][0] < 230 and matrix[i,j][3] > 0):
            coastline.append((i,j, matrix[i,j][0]))
newCoastline = []

def lambert_cylindrical_equal_area():
    global newCoastline
    for i in range(len(coastline)):
        latitude = (5000-coastline[i][1])/5000*90
        newCoastline.append((coastline[i][0],
sin(radians(latitude))*5000+5000, coastline[i][2]))

def mercator():
    global newCoastline
    for i in range(len(coastline)):
        latitude = (5000-coastline[i][1])/5000*90
        if abs(latitude) > 85:
            continue
        constant =
round(log(abs(1/cos(radians(latitude))+tan(radians(latitude)))))*
5000/3.13130133147)
        if constant > 5000:
            constant = 5000
        elif constant < -5000:
            constant = -5000
        newCoastline.append((coastline[i][0], constant+5000, coas-
tline[i][2]))

def central_cylindrical():
    global newCoastline
    for i in range(len(coastline)):
        latitude = (5000-coastline[i][1])/5000*90
        if abs(latitude) > 66.5:
            continue
        constant = round(tan(radians(latitude))*5000/2.29984254724)
        if constant > 5000:
            constant = 5000
        elif constant < -5000:
            constant = -5000

```

```

        newCoastline.append((coastline[i][0], constant+5000,
coastline[i][2]))

def equal_earth():
    A1 = 1.340264
    A2 = -0.081106
    A3 = 0.000893
    A4 = 0.003796
    maxX = -infy
    maxY = -infy
    minX = infy
    minY = infy
    for i in range(len(coastline)):
        latitude = (5000-coastline[i][1])/5000*90
        longitude = ((coastline[i][0]-10000)/10000*180)
        theta = arcsin(sqrt(3)/2*sin(radians(latitude)))
        x =
round(( (2*sqrt(3)*longitude*cos(theta))/(3*((9*A4*theta**8)+(7*A3*
theta**6)+(3*A2*theta**2)+A1)))*10000/155.07847476934788+10000)
        y =
round((A4*theta**9+A3*theta**7+A2*theta**3+A1*theta)*5000/1.317362
759157413+5000)
        newCoastline.append((x, y, coastline[i][2]))

mercator()

newMatrix = [[(255,255,255,255) for j in range(10001)] for i in
range(20001)]
for i in newCoastline:
    pixel = min(newMatrix[i[0]][10000-i[1]][0], i[2])
    newMatrix[i[0]][10000-i[1]] = (pixel, pixel, pixel, 255)
# Create a new image from newMatrix
new_map = Image.new('RGBA', (20001, 10001))
for i in range(10001):
    for j in range(20001):
        new_map.putpixel((j, i), newMatrix[j][i])
new_map.save('/Users/kunshansun/Downloads/Mercator.png')

```

Here are the typical images produced after thickening the lines with a separate Python program: (**Figure 1** and **Figure 2**).



**Figure 1.** The Mercator projection, a well-known projection, generated by the PIL Python package up to approximately 80° latitude.

2.2. Methods

The next snippet of code uses a divide-and-conquer algorithm to break up the specified area into 4 equally sized boxes during every iteration and then count the number of boxes covered by coastline at each iteration. These results will be used to calculate the fractal dimension of the piece of coastline in question using the box-counting method. The results, which come as a list of the number of boxes counted for several box sizes ( $512 \times 512$ ,  $256 \times 256$ , ...,  $1 \times 1$ ), are then fed into Desmos using a table. The logarithm of both columns is then recorded. Next, the “box sizes” column is reversed, denoting a  $512 \times 512$  box size as entry 0, a  $256 \times 256$  box size as entry 1, and so on. The least-squares regression line is then calculated, and the slope is recorded as the fractal dimension (Figure 3).

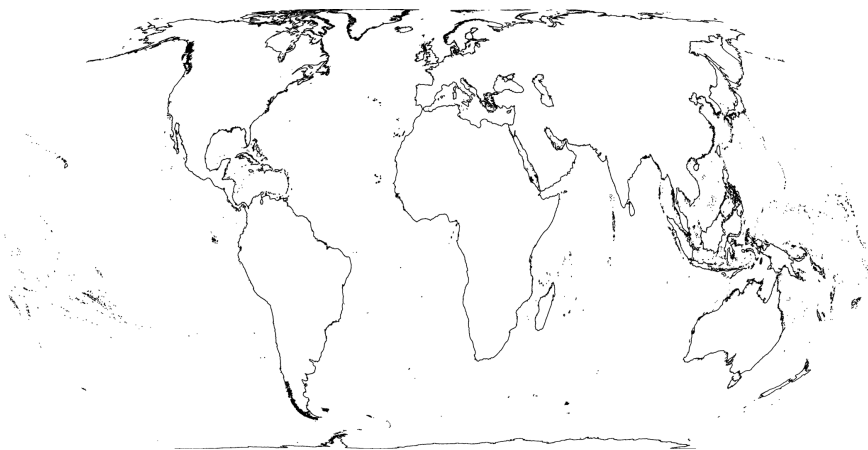


Figure 2. The Equal Earth Projection, generated by the PIL Python package.

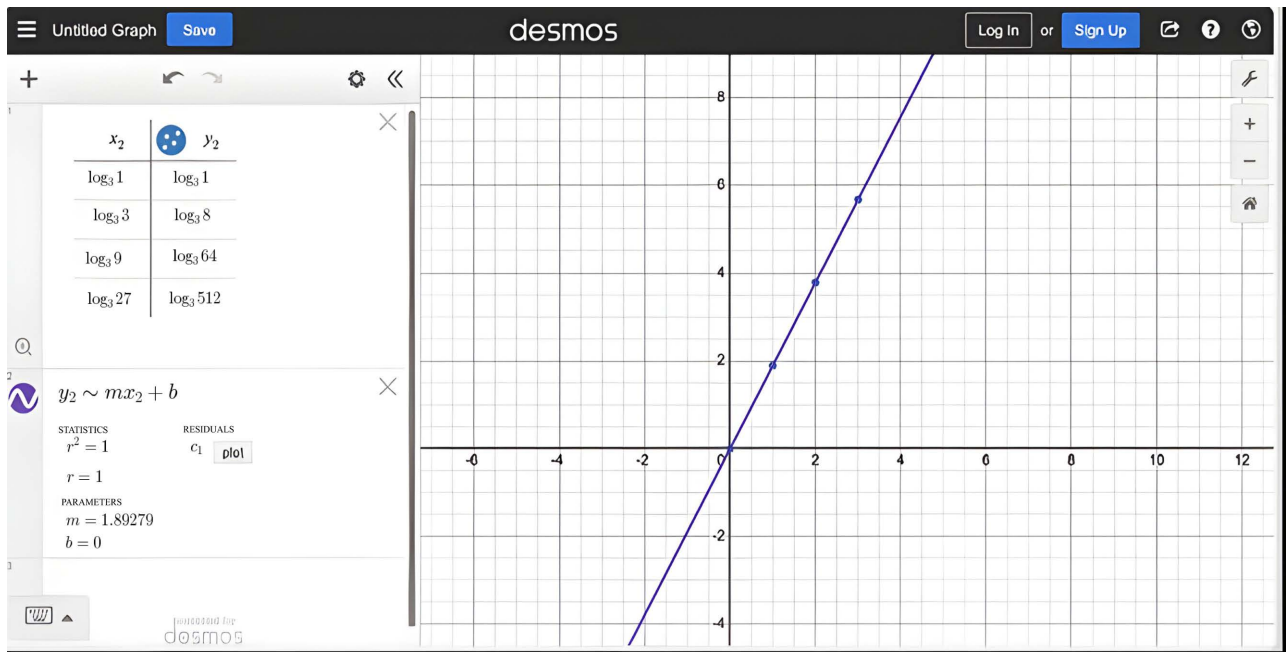


Figure 3. A sample linear regression to find the fractal dimension of the Sierpinski Carpet. Note that the number of boxes on each side of the bounding box triples instead of doubles with each iteration.

The code below implements this method, and the outputs for different bounding boxes and different projections are compared.

```
# Formulas from [1]

from matplotlib import *
from pylab import *
from PIL import Image
from numpy import log2

Image.MAX_IMAGE_PIXELS = 200030001

map = Image.open('/Users/kunshansun/Downloads/lines (2).png')
matrix = map.load()
boxCounts = [0 for i in range(10)]

def set_box_counts(x1, y1, x2, y2, coastline):
    global boxCounts
    coastlines = [[] for i in range(4)]
    if coastline[0] == (-1, -1):
        coastline = []
        for i in range(x1, x2 + 1):
            for j in range(y1, y2 + 1):
                if (matrix[i, j][0] < 100):
                    coastline.append((i, j))
    if x1 == x2 and y1 == y2:
        # Will only test square regions with side lengths that are powers
        # of 2 pixels in length
        if (matrix[x1, y1][0] < 100):
            boxCounts[0] += 1
            return 1
        else:
            return 0
    for i in coastline:
        if i[0] <= (x1 + x2) // 2:
            if i[1] <= (y1 + y2) // 2:
                coastlines[0].append(i)
            else:
                coastlines[1].append(i)
        else:
            if i[1] <= (y1 + y2) // 2:
                coastlines[2].append(i)
            else:
                coastlines[3].append(i)
    sum = 0
    sum += set_box_counts(x1, y1, (x1+x2)//2, (y1+y2)//2, coastline) + \
        set_box_counts((x1+x2)//2+1, y1, x2, (y1+y2)//2, coastline) + \
        set_box_counts(x1, (y1+y2)//2+1, (x1+x2)//2, y2, coastline) + \
        set_box_counts((x1+x2)//2+1, (y1+y2)//2+1, x2, y2, coastline)
    if sum > 0:
        boxCounts[int(log2(abs(x2 - x1) + 1))] += 1
    return sum

set_box_counts(5571, 9305, 5571 + 511, 9305 + 511, [(-1, -1)])
print(*boxCounts) # I did an analysis of the boxCounts list outputted
using a log-log regression on Desmos.
```

To ensure a fair comparison between map projections, I recorded measurements of fractal dimensions for both the Equirectangular and Mercator projections in medium-high latitude regions.

### 3. Results and Discussion

Below is a table analyzing the fractal dimensions of pieces of coastlines enclosed



in fixed 512 by 512-pixel boxes centered at different geographic regions. Note that the box-counting method may produce results biased towards higher values.

Looking at the data for the regions where the Mercator projection has extreme distortion ( $\geq 70^\circ$  latitude), there is a noticeable difference in the fractal dimension between the equirectangular projection and the Mercator projection when the bounding box for the coastline is fixed and centered at the same geographic area. Regions closer to the equator ( $\leq 60^\circ$  latitude) tend to result in negligible differences, with less variability between projections. Nevertheless, the differences can still be detected in these regions.

The differences in fractal dimension between the Mercator and Equirectangular projections are dependent on the nature of the coastline in the region examined. Since the fractal dimension is a measure of the length of coastlines, the more coastline in a bounding box, the higher the fractal dimension should be [8]. This is exemplified by northern Norway's coastline because the Mercator projection stretches vertically near the poles, causing the small promontories on the horizontal coastline to be stretched while not becoming larger than the bounding box. This would increase the length of the coastline contributed by those vertical features, so the fractal dimension goes up by a noticeable amount. Northern Norway is known for its complex coastline, as shown in **Figure 4**. In the Mercator Projection, on areas of coastline extending from east-west, small coastal features will be stretched north-south, which increases the apparent length of the coastline. However, this stretching would not cause the coastal features to extend outside of the bounding box, but this would significantly increase the length of northern Norway's coastline. Therefore, the fractal dimension of northern Norway would increase from the Equirectangular to the Mercator projection, specifically an increase of approximately  $\frac{1.5361 - 1.4748}{1.4748} \times 100\% \approx 4.1565\%$ . This increase signifies that the Mercator Projection increases the degree of complexity of the coastline in this region.

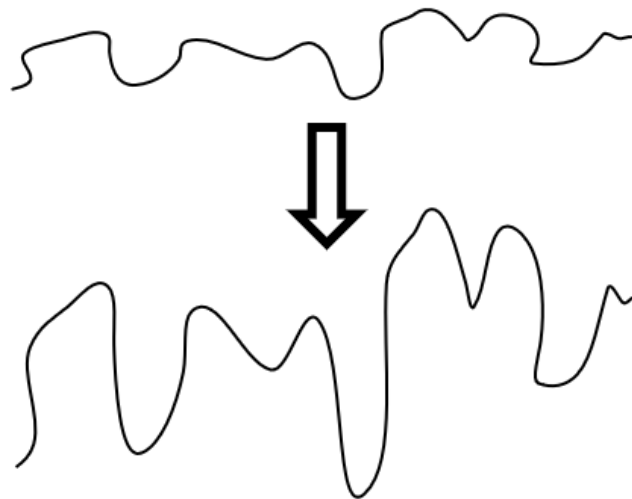


**Figure 4.** A horizontal coastline that is stretched vertically during projection.

Northeastern Greenland's coastline, on the other hand, is mainly vertical with horizontal features, so the original coastline contained within the bounding box would be stretched beyond the boundaries of the box when using the Mercator projection. Since the horizontal features do not get stretched horizontally by a significant amount, the overall length of the coastline that is contained within the fixed-sized and fixed-location bounding box decreases as its complexity decreases. Features at the extreme north and south of the bounding box exit, which is exemplified by **Table 1** and **Figure 5**. In other words, in the Mercator projection, on stretches of coastline running north-south, small coastal features that point in the east-west direction get stretched vertically, or in the north-south direction. This stretching causes some coastal features to exit the original bounding box, which doesn't change in size, according to location in terms of GPS coordinates. The loss of these coastal features decreases the length of the coastline in the bounding box. Since the fractal dimension is directly correlated with the length of the coastline in an area, the fractal dimension decreases, specifically by a factor of  $\frac{1.6140 - 1.4847}{1.6140} \times 100\% \approx 8.0112\%$ .

The southwestern corner of the Antarctic Peninsula, shown in **Figure 6**, is more complicated because it combines horizontal and vertical coastlines. However, since the peninsula's coastline has more vertical changes, the fractal dimension for the Mercator projection is slightly lower than that of the Equirectangular projection. As shown in the figure below, the Mercator projection significantly stretches the vertical features, which are denoted by the rightmost purple line segment. The mainly horizontal stretch of coastline in the center of the figure, though, doesn't deviate much from the main line that the coastline follows, as denoted by the centermost blue segment. This means that the vertical stretches of coastline are affected the most by the Mercator projection, causing some of their features to leave the bounding box. This decreases the length of the coastline inside the bounding box, which decreases the fractal dimension of the coastline enclosed in the bounding box.

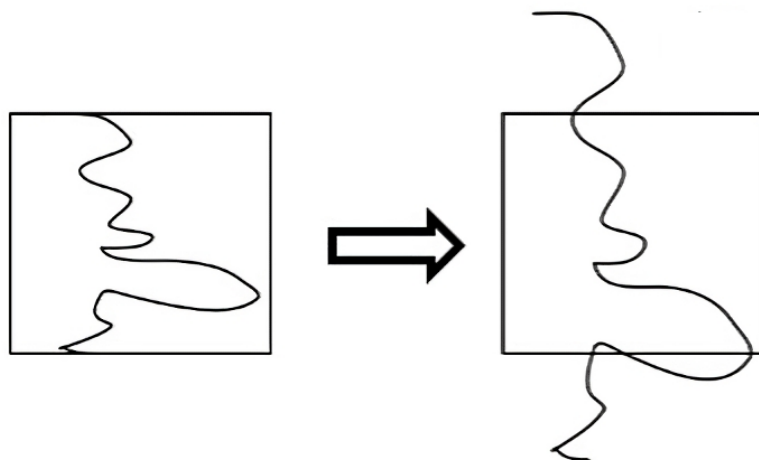


**Figure 5.** A vertical coastline that is stretched vertically during projection.

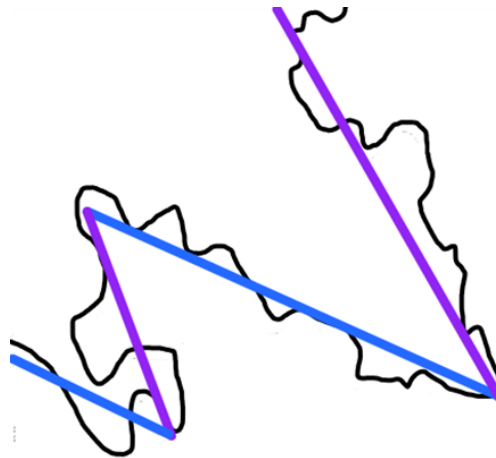


**Figure 6.** A representation of the southwestern end of the Antarctic Peninsula, where it meets the mainland. The purple stretches of the coastline are nearly vertical, and the blue stretches are nearly horizontal.

**Table 1.** Fractal dimensions were calculated using the Mercator and Equirectangular projections at five different geographical areas.

| Region   | Fractal Dimension   |                            |
|--|---------------------|----------------------------|
|  | Mercator Projection | Equirectangular Projection |
| Northern Norway: High Latitude, Horizontal Coastline                           | 1.5361              | 1.4748                     |
| Southwestern Greenland: Medium-High Latitude, Vertical Coastline               | 1.5832              | 1.5917                     |
| Northeastern Greenland: High Latitude, Vertical Coastline                      | 1.4847              | 1.6140                     |
| Northern Tip of the Antarctic Peninsula: Medium-High Latitude, Mixed Coastline | 1.5362              | 1.5240                     |
| Southwestern Antarctic Peninsula: High Latitude, Mixed Coastline               | 1.3558              | 1.4055                     |

Similarly comparing stretches of horizontally aligned coastlines and vertically aligned coastlines projected with the Equirectangular projection and other projections, we can determine the main direction that the map stretches or compresses different areas, even if that direction is neither perfectly horizontal nor vertical.

4. Conclusions

In this study, we used fractal dimension changes of coastlines in different regions of the world to quantify the distortion of two common map projection methods: the Mercator Projection and the Equirectangular Projection. We further analyzed how the two map projections affected the fractal dimension of

coastlines. As a geometric property, fractal dimension can not only compare changes in regions with extreme distortions but can also compare the degree of distortion in regions with only slight distortions, such as the mid-latitude regions. Moreover, this method uses the fractal dimension of *coastlines*, but it is not limited to regions close to the sea. Using changes in the fractal dimensions of different shapes, we can easily examine distortions on inland regions using any geographic features that are self-similar to some degree such as mountain ranges, rivers, and city limits. For example, to examine terrestrial features that extend for thousands of miles, such as the Rocky Mountain Range, the Andes, and the Mid-Atlantic Ridge, it is essential to know which directions map projections distort geographic features and the areas where maps distort the most. Topographic maps, which are graphed on 3-D space, are defined based on a 2-D map (the  $x$  and  $y$  axes), with elevation or another geographic property plotted on the  $z$ -axis. This relation between map projections and the graphing of geomorphic features makes quantifying map projection distortion, especially finding areas (typically lines of latitude or longitude) where distortion is minimal, an integral part of geomorphology [17].

Using fractal dimension to quantify map projection distortion inherently offers notable advantages by enhancing measurement precision and objectivity. It also enables comprehensive deformation analysis across diverse environments, including topographic maps. The box-counting method, identified as an efficient technique for calculating fractal dimensions, further contributes to the study's robustness with its ease of implementation, rapid processing of large datasets, and flexible parameter adjustments. This study underscored the significance of considering the effects of map projections on the fractal dimensions of coastlines, which fuels future research to explore the mechanisms underlying different projections' impacts on coastline morphology and the potential applications of fractal dimension in cartography, geographic information science, and geomorphology.

Additionally, the usage of fractal dimensions to quantify map projection distortion focuses on shape distortion in general rather than distortions of single elements such as angles or areas. Thus, it is a high-level measurement tool for map projection evaluation and provides a universal tool to compare hundreds of projection methods created for different purposes. With the development of satellite imaging and remote sensing technology, more precise and complete data of surface morphologies are in development and become more easily accessible. This constructs a basis for the wider application of the fractal dimension quantification method. The method is also versatile and can be used to quantify geometric changes in other contexts, such as the evolution of mountain ranges or even galaxies over time.

Although this is a novel way of finding the degree of distortion of map projections, it also has its limitations. Compared to other methods of evaluating map projection distortion, the box-counting method on different stretches of coas-

tline takes more computational power than directly finding the distortion of geometric properties using known mathematical formulas, since the box-counting method involves recursion and regression. Another potential downside to this method is that the box-counting method is sensitive to many types of parameters, especially the box sizes that are chosen for comparison. The type of coastline could also affect the result, as a box can get counted even if it has only a tiny stretch of coastline in it [18]. Moreover, the resulting fractal dimension could be affected by the quality of the images that are processed. Nevertheless, most of the insufficiencies stated above can be fixed by performing many different trials in many different regions to ensure a more accurate and broad comparison.

Further research should be conducted to eliminate the negative effects of poor image quality using different types of fractal dimension calculation methods, including the walking divider dimension proposed by Lewis F. Richardson. Research should also be done to develop a standard model for all the world's coastlines, perhaps by shifting latitude lines to ensure that the queried region is near a standard parallel or a latitude where the map projection doesn't incur any distortion [19]. Future researchers could also collect data on more regions to examine the effects of angular distortion within a specified bounding box. Furthermore, research should be conducted regarding the applicability of analyzing changes in fractal dimension in other types of images such as landscapes and MRI scans.

## Conflicts of Interest

The author declares no conflicts of interest regarding the publication of this paper.

## References

- [1] Ward, M.O., Grinstein, G. and Keim, D. (2010) Interactive Data Visualization: Foundations, Techniques, and Applications. CRC Press, New York.  
<https://doi.org/10.1201/b10683>
- [2] Mulcahy, K.A. and Clarke, K.C. (2001) Symbolization of Map Projection Distortion: A Review. *Cartography and Geographic Information Science*, **28**, 167-182.  
<https://doi.org/10.1559/152304001782153044>
- [3] Arasan, S., Akbulut, S. and Hasiloglu, A.S. (2011) The Relationship between the Fractal Dimension and Shape Properties of Particles. *KSCE Journal of Civil Engineering*, **15**, 1219-1225. <https://doi.org/10.1007/s12205-011-1310-x>
- [4] Cheng, Q. (1995) The Perimeter-Area Fractal Model and Its Application to Geology. *Mathematical Geosciences*, **27**, 69-82. <https://doi.org/10.1007/BF02083568>
- [5] Smith, H.J.S. (1874) On the Integration of Discontinuous Functions. *Proceedings of the London Mathematical Society*, s1-6, 140-153.  
<https://doi.org/10.1112/plms/s1-6.1.140>
- [6] Koch, H. (1904) Sur une courbe continue sans tangente, obtenue par une construction géométrique élémentaire. *Arkiv för matematik, astronomi och fysik*, **1**, 681-704.
- [7] Richardson, L.F. (1961) The Problem of Contiguity: An Appendix to Statistics of

- Deadly Quarrels. <https://api.semanticscholar.org/CorpusID:58813091>
- [8] Mandelbrot, B. (1967) How Long Is the Coast of Britain? Statistical Self-Similarity and Fractional Dimension. *Science*, **156**, 636-638. <https://doi.org/10.1126/science.156.3775.636>
  - [9] Mandelbrot, B.B. and Mandelbrot, B.B. (1982) The Fractal Geometry of Nature. W. H. Freeman and Co., New York.
  - [10] Sanchez, N., Alfaro, E.J. and Perez, E. (2005) The Fractal Dimension of Projected Clouds. *The Astrophysical Journal*, **625**, 849-856. <https://doi.org/10.1086/429553>
  - [11] Bearer, E.L., Medina, C.S., Uselman, T.W. and Jacobs, R.E. (2023) Harnessing Axonal Transport to Map Reward Circuitry: Differing Brain-Wide Projections from Medial Prefrontal Cortical Domains. *Frontiers in Cell and Developmental Biology*, **11**, Article ID: 1278831. <https://doi.org/10.3389/fcell.2023.1278831>
  - [12] Burrough, P.A. (1981) Fractal Dimensions of Landscapes and Other Environmental Data. *Nature*, **294**, 240-242. <https://doi.org/10.1038/294240a0>
  - [13] Chen, Y., Wang, J. and Feng, J. (2017) Understanding Fractal Dimension of Urban Form through Spatial Entropy. *Entropy*, **19**, Article 600.
  - [14] Husain, A., Reddy, J., Bisht, D. and Sajid, M. (2021) Fractal Dimension of Coastline of Australia. *Scientific Reports*, **11**, Article No. 6304. <https://doi.org/10.1038/s41598-021-85405-0>
  - [15] Wu, J., Jin, X., Mi, S. and Tang, J. (2020) An Effective Method to Compute the Box-Counting Dimension Based on the Mathematical Definition and Intervals. *Results in Engineering*, **6**, Article ID: 100106. <https://doi.org/10.1016/j.rineng.2020.100106>
  - [16] OpenStreetMap contributors, "coastlines-split-4326". <https://osmdata.openstreetmap.de/data/coastlines.html>
  - [17] Lemenkova, P. and Debeir, O. (2023) Quantitative Morphometric 3D Terrain Analysis of Japan Using Scripts of GMT and R. *Land*, **12**, Article 261. <https://doi.org/10.3390/land12010261>
  - [18] Miloevic, N.T., Rajkovic, N., Jelinek, H.F. and Ristanovic, D. (2013) Richardson's Method of Segment Counting versus Box-Counting. 2013 19th International Conference on Control Systems and Computer Science, Bucharest, 29-31 May 2013, 299-305. <https://doi.org/10.1109/CSCS.2013.52>
  - [19] Lapaine, M. (2023) On the Definition of Standard Parallels in Map Projections. *ISPRS International Journal of Geo-Information*, **12**, Article 490. <https://doi.org/10.3390/ijgi12120490>